Epilepsy Research 149 (2019) 117–122

Contents lists available at ScienceDirect

Epilepsy Research

journal homepage: www.elsevier.com/locate/epilepsyres

Conductive gel bridge sensor for motion tracking in simultaneous EEG-fMRI recordings

Noa Cohen[a,d,*], Evgeny Tsizin[e], Itzhak Fried[c,d], Firas Fahoum[b,d], Talma Hendler[a,d], Tomer Gazit[a,1], Mordekhay Medvedovsky[a,1]

[a] Sagol Brain Institute, Tel Aviv Sourasky Medical Center, Tel Aviv, Israel
[b] Epilepsy and EEG Unit, Department of Neurology, Tel Aviv Sourasky Medical Center, Tel Aviv, Israel
[c] Functional Neurosurgery Unit, Tel Aviv Medical Center, Tel Aviv, Israel
[d] Sackler School of Medicine, Tel Aviv University, Tel Aviv, Israel
[e] School of Electrical Engineering, Tel Aviv University, Tel Aviv, Israel

ARTICLE INFO

Keywords:
EEG-fMRI
Epilepsy
Motion artifact
Motion sensor
Conductive gel bridge

ABSTRACT

EEG-fMRI allows the localization of the hemodynamic correlates of neural activity and has been shown to be useful as a diagnostic tool in pre-surgical evaluation of refractory epilepsy. However, EEG recordings may be highly contaminated by artifacts induced by movements inside the magnetic field thus rendering the scan difficult for interpretation. Existing methods for motion correction require additional equipment or hardware modification. We introduce a simple method for motion artifact detection, the conductive gel bridge sensor (CGBS), easily applicable using the standard setup. We report examples of CGBS use in two patients with epilepsy and demonstrate the method's ability to successfully differentiate between epochs of brain activity and those of movement.

1. Introduction

Electroencephalography combined with functional magnetic resonance imaging (EEG-fMRI) is a neuro-imaging method which combines the high temporal resolution of EEG and the high spatial resolution of fMRI. An important application of EEG-fMRI is in epilepsy presurgery workup in which fMRI is used to localize the hemodynamic correlate of interictal epileptiform discharges (IEDs), providing information regarding the location of the seizure onset zone (SOZ; Warach et al., 1996; Gotman, 2008). One of the substantial obstacles for this method is motion interference, which is a result of small-amplitude head and cable movements inside a strong magnetic field. To detect such movements, several types of sensors, which track motion independently from the EEG signals, were developed. The piezoelectric sensor attached to the temporal artery area was reported by Bonmassar et al. (2002), Masterton et al. (2007) and Abbott et al. (2014) described wire loops fixed to the EEG cap; reference layer electrodes were used by Luo et al. (2014) and Chowdhury et al. (2014). Körbl et al. (2016) and Maziero et al. (2016) employed optic recordings for motion sensing. One previous study reported that components of the EEG array itself may serve as a motion sensor when the electrodes are interconnected by a cable (Jorge et al., 2015). However, these methods require additional MR-compatible equipment or EEG setup modifications.

In this short report we introduce the conductive gel bridge sensor (CGBS), which is based on EEG electrode interconnection through a simple gel bridge. This creates a loop, which is short-circuited from the scalp, and can serve as an efficient motion sensor without the need for additional hardware or EEG array modification.

2. Methods

2.1. Patients and acquisition

Two patients with refractory epilepsy underwent EEG-fMRI scans using the dual array EEG (daEEG) method with an oblique-bundled cap (Klovatch-Podlipsky et al., 2016). The study was approved by the Tel-Aviv Sourasky Medical Center Ethical Review Board. Written informed consent for participation in the study was obtained from the two patients.

MRI scans were performed in a 3.0 T MRI scanner with a 20-channel

Abbreviations: CGBS, conductive gel bridge sensor; daEEG, dual array electroencephalogram

* Corresponding author at: Sagol Brain Institute, Tel Aviv Sourasky Medical Center, 6 Weisman st., 64239, Tel-Aviv, Israel.
E-mail address: noahcohen@tauex.tau.ac.il (N. Cohen).

[1] Authors contributed equally to the work.

https://doi.org/10.1016/j.eplepsyres.2018.12.008
Received 4 June 2018; Received in revised form 27 November 2018; Accepted 17 December 2018
Available online 17 December 2018
0920-1211/

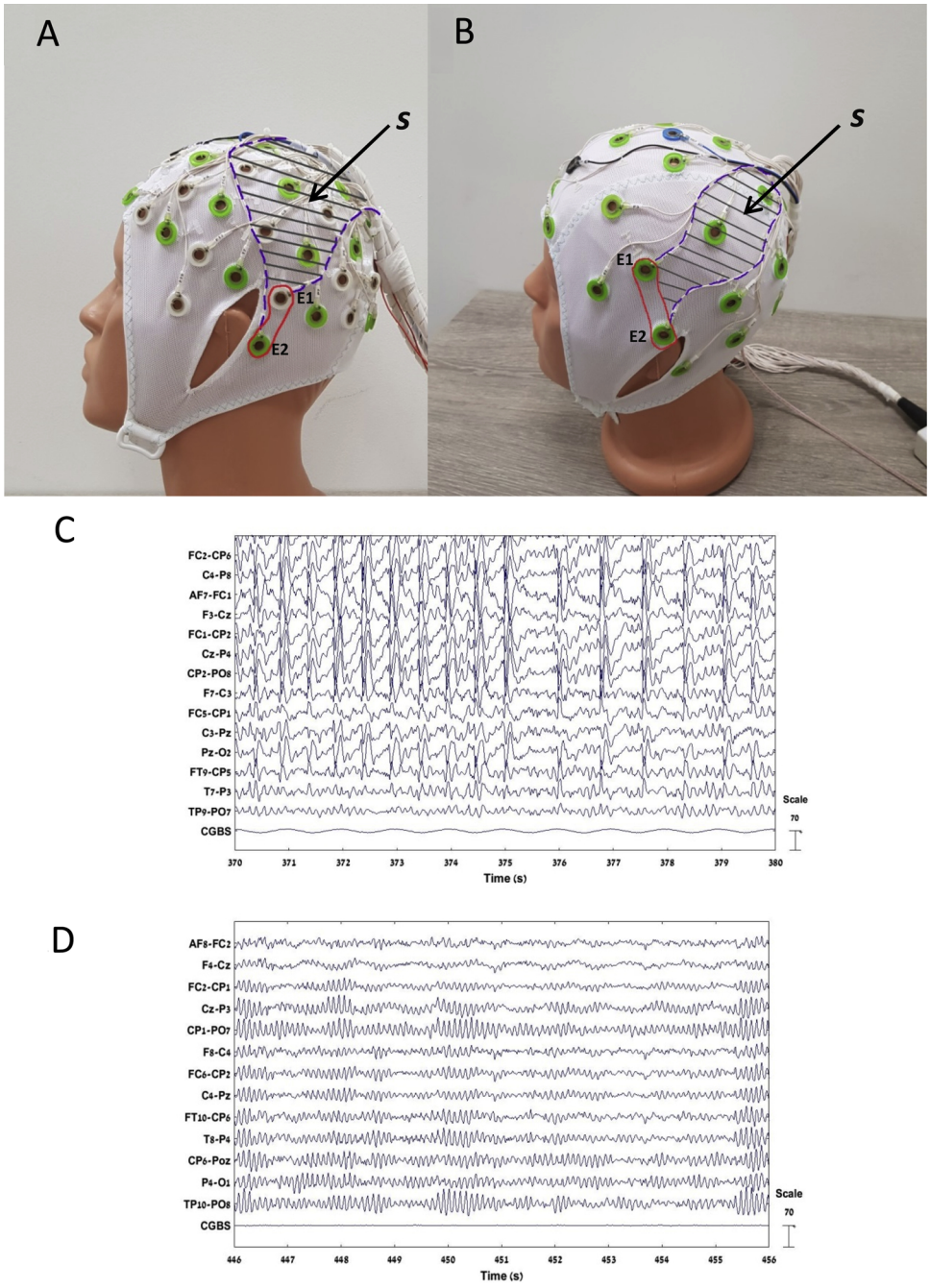

Fig. 1. Examples of the CGBS configuration and bipolar representation of a recording sample obtained outside of the MR scanner. 1 A &B: Red line marks the gel bridge between two electrodes E1 and E2. Purple dotted lines correspond to two cables connected to the gel bridge electrodes creating an electromagnetic induction loop, the area S of which is marked by parallel grey lines. (Fig 1A) Dual array 64 channel cap (Fig. 1B) Standard 32 channel EEG cap (Brain products). 1C&D: The bridged electrode pair (last channel) shows no trace of brain activity and no BCG artifact in both patients during either a sequence of spike-and-wave complexes in Patient 1 (Fig. 1C) or background rhythmic alpha activity in Patient 2 (Fig. 1D). The slow oscillation seen on the CGBS in Fig. 1C likely results from a non-biological source such as the ambient electromagnetic field or electronic noise from the amplifiers. MT, magnetic resonance; CGBS, conductive gel bridge sensor.

head receiver coil. A T2*- weighted, gradient echo, echo planar imaging (EPI) sequence was used for recording the fMRI images. EEG acquisition protocol and artifact removal were previously described (Klovatch-Podlipsky et al., 2016). In this case the recording length was 10 min and the number of recording sessions, was between 6 and 8.

To create a conductive gel bridge in the EEG, the experimenter inserted a large quantity of gel such that it created a link between two adjacent electrodes in the daEEG cap, located far from the area of the expected IED field as determined by previously recorded video EEG. Data from the bridged electrode pair underwent ballistic cardiogram (BCG) artifact removal using the optimal basis set (OBS; Luo et al., 2014) method implemented with the FMRIB plug-in for EEGLAB, provided by the University of Oxford Centre for Functional MRI of the Brain (Niazy et al., 2005; Iannetti et al., 2005; Smith, 2002).

The EEG data (but not the CGBS trace) were first denoised using the dual array EEG approach (Klovatch-Podlipsky et al., 2016). This approach assumes that brain-generated signals do not depend on the cable arrangement over the scalp, whereas motion-generated artifacts do. To this end, EEG recorded inside the MR-scanner is initially decomposed by independent component analyses (ICA) and later the denoised EEG is reconstructed from the components whose spatial distribution does not depend on the cable arrangement.

Next, to differentiate between motion artifacts, which still remained after dual array denoising, and genuine brain generated EEG waveforms, the bipolar measurement of the bridged trace (both unprocessed and processed by OBS) was added to the EEG traces of the non-bridged pairs.

The traces were viewed by a neurologist (MM) who manually marked IEDs. These events were used to analyze the fMRI data in an event related General Linear Model (GLM) design using SPM12 (http://www.fil.ion.ucl.ac.uk/spm). Preprocessing included slice timing correction, 3D motion correction and co-registration to the anatomical

image. The data was smoothed spatially with an 8 mm full width at half maximum (FWHM) Gaussian kernel. To account for motion artifacts and outliers, the Artifact Detection Tools (ART) toolbox (https://www.nitrc.org/projects/artifact_detect/) was applied adding 6 movement regressors as well as an additional regressor for each detected outlier.

For assessment of the role of CGBS in IED detection, a second neurologist (FF), blinded to the initial results, was asked to mark artifacts, IEDs and non-epileptic brain transients: first without and then

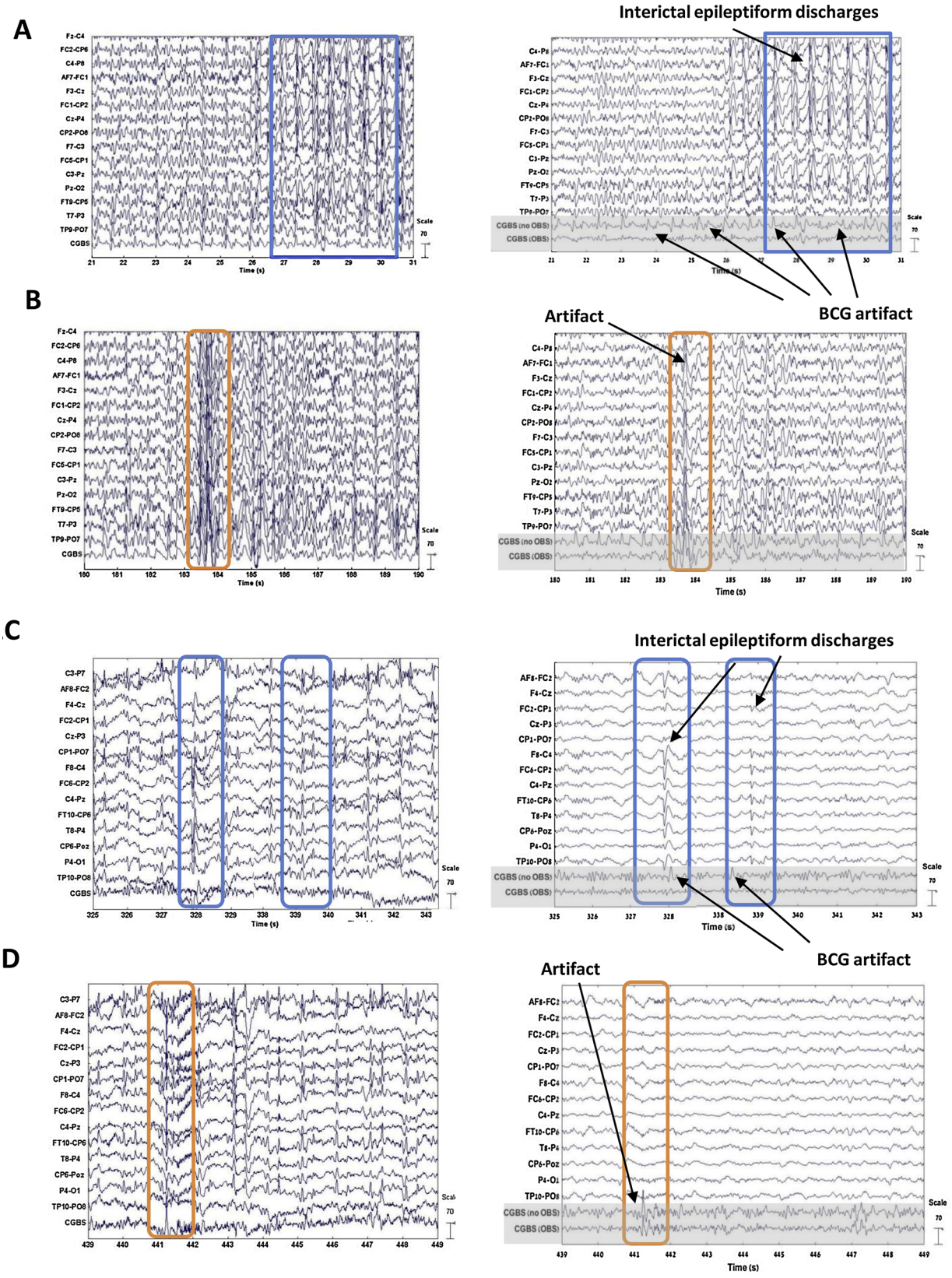

(caption on next page)

Fig. 2. Bipolar representation of EEG recordings from two patients inside the MR scanner with manually added CGBS traces. Left column shows the same recording segment as in the right, before application of cleaning techniques (see methods). 2 A&B correspond to Patient 1 and 2C&D to Patient 2. Blue rectangles mark epochs of IEDs and orange rectangles mark epochs of artifacts without IEDs. The CGBS recording in the right column is shown in the two lowermost channels: second to last channel shows the CGBS as recorded without additional processing and last channel shows the CGBS after OBS application. In Fig. 2A BCG waveforms, but not IEDs, are clearly seen before and during the IED burst on the CGBS channels, mainly before OBS application. Fig. 2C shows two instances of single spikes with no corresponding activity on the CGBS. Again, BCG artifacts can be seen on CGBS channels, mainly before OBS, but not on EEG channels due to successful cleaning by the dual array method. In 2B arrow points to artifacts on the EEG trace captured both on the CGBS channel and the other EEG channels, not successfully cleaned with the dual array approach. In 2D an artifact is seen on the CGBS but hardly seen on the EEG channels (due to successful cleaning by the dual array method). MR, magnetic resonance; CGBS, conductive gel bridge sensor; IEDs, interictal epileptiform discharges; OBS, optimal basis set; BCG, ballistic cardiogram.

with the use of the CGBS trace, in 20-minute segments of the in-scanner EEG recordings of both patients. He was also asked to indicate whether the type of individual electrographic events can be defined with certainty. Thus, the events were classified into 6 categories: artifacts (certain/uncertain), IEDs (certain/uncertain) and non-epileptic brain transients (certain/uncertain). BOLD activation maps in response to the certain IEDs marked before and after CGBS use were generated and compared.

Additionally, in order to evaluate whether CGBS can also be used to improve fMRI mapping by including outlier time points in the analysis, we calculated the Root Mean Square (RMS) of the CGBS channel during each TR (3 s) and detected TRs during which the RMS measure exceeded 5 standard deviations about the mean. These timepoints were considered as outliers each to be inserted as a regressor instead of the ART outlier regressors (in addition to the IED and movement regressors). The resulting T-maps were compared to those using ART and those without any outlier regressors added to the GLM.

2.2. Theoretical framework

The motion of the CGBS loop causes a change in the magnetic flux $\int_S \mathbf{B}\cdot d\mathbf{A}$, where B denotes the constant magnetic field of the MR system, S is the surface area delimited by the loop and dA is a differential element of S. This flux change induces a voltage $V_{E1E2,motion}$:

$$V_{E1E2,motion} \sim -\frac{d}{dt}\left(\int_S \mathbf{B}\cdot d\mathbf{A}\right).$$

Another additive component of the voltage V_{E1E2} measured on the same electrodes $E1E2$ is related to the neural activations within the brain. We denote this component by $V_{E1E2,neural}$.

$V_{E1E2,neural}$ can be calculated from the voltage inside the epidermis in close proximity to the electrodes $E1E2$ which is denoted by $V_{epidermis,E1E2}$. Its value is of the order of $100\mu V$. Since $V_{epidermis,E1E2}$ is divided between the electrode/skin contact impedance $R_C \approx 5k\Omega$ and the impedance of the gel bridge $R_{CGBS} \approx 5\Omega$, the voltage $V_{E1E2,neural}$ can be calculated as follows:

$$V_{E1E2,neural} = V_{epidermis,\,E1E2}\frac{R_C}{R_C + R_{CGBS}} < \approx 100\mu V\cdot\frac{5\Omega}{5\Omega + 5k\Omega} \approx 0.1\mu V$$

This voltage is significantly lower than the EEG amplitude and can be neglected relative to the $V_{E1E2,motion}$; $V_{E1E2} = V_{E1E2,neural} + V_{E1E2,motion} \approx V_{E1E2,motion}$

As a result, the overall voltage between the electrodes $E1E2$ can be considered as a motion indicator.

3. Results

The trace of the bridged electrode pair was nearly flat when recorded outside of the MR-scanner, meaning that no brain activity was recorded (Fig. 1C,D). Inside the scanner the bridged pair demonstrated a BCG artifact and other deflections corresponding to head\cable motion (Fig. 2). Before application of the dual array artifact suppression approach, the EEG channels contained motion artifacts mixed with EEG signals, while CGBS – only motion artifacts (Fig. 2B,D). After dual array approach application, most of the motion artifact had been suppressed and its residuals could easily be identified by superposition with CGBS (Fig. 2D). OBS for pulse artifact removal reduced part of the BCG artifact. IEDs were not associated with deflections in the bridged electrode pair trace. Patient 1 showed a diffuse pattern of epileptiform spike-and-wave sequences (Fig. 2A) on EEG while the CGBS at the same time showed no change. In a second time-window a spike-like motion artifact can be seen clearly correlated to the CGBS signal, preventing the misinterpretation of this artifact as an IED (Fig. 2B). In the EEG of Patient 2, individual IEDs are not associated with any signal change on the CGBS (Fig. 2C) while motion artifacts, which were mostly cleaned by the daEEG approach, appeared like spikes on the CGBS (Fig. 2D).

Markings done by the second neurologist on two example sessions for each patient with CGBS revealed a 38% and 60% increase in certainty of IED identification for patients 1 and 2 respectively, compared to marking without CGBS (Full results are in Supplementary Table 1). These corresponded to higher peak t values after CGBS use (t = 3.18, t = 2.6) in the presumed seizure onset zone of the patients (as assessed using video-EEG), when compared to the same areas before CGBS use (t = 2.85, t = 0.9; Supplementary Fig. 1)

CBGS and ART detected mostly the same TRs with head motion (Supplementary Fig. 2). CGBS based movement outlier regressors added to the analysis process resulted in BOLD maps similar to those produced using the ART regressors, with comparable t values (Fig. 3). Both regression methods seem to improve results compared to the standard GLM analysis, which does not consider motion outliers (Table 1).

4. Discussion

In this short report, we demonstrate that a simple gel bridge between two adjacent electrodes can create an efficient motion sensor in EEG-fMRI, which is sensitive to head motion and insensitive to the electric field originating from the brain. Gel bridges are relatively common in EEG-fMRI and they do not compromise patient or device safety.

Here we intentionally created a gel bridge in a controlled manner. In contrast to existing motion sensors (Bonmassar et al., 2002; Masterton et al., 2007; Abbott et al., 2014; Luo et al., 2014; Chowdhury et al., 2014; Jorge et al., 2015; Körbl et al., 2016; Maziero et al., 2016), the CGBS requires neither additional software, nor a change in the EEG electrode array. Closer electrodes in a dense arrangement such as in the 64-electrode array (Fig. 1A) allow for an easier application of the CGBS, however it can also be used with a 32-channel system (Fig. 1B). In this study we first used daEEG (Klovatch-Podlipsky et al., 2016) which allows suppression of the main bulk of motion interference and later our newly developed CGBS method to distinguish brain signals (such as IEDs) from motion artifact residuals (Fig. 2).

According to our study, CGBS increases the certainty of EEG event identification, which can be translated into better delineation of fMRI hemodynamic correlates of these events (supplementary Fig. 1). CGBS can also be used to detect motion outliers and improve statistical power of BOLD similarly to fMRI based methods, such as ART (Fig. 3).

A downside to using CGBS is that the bipolar EEG pairs used in the CGBS cannot be used for the EEG recording itself. However, we believe that this is a justified cost, especially with a 64-electrode (or higher) array and when the CGBS location is chosen far from the expected IED field. Another issue is that the trace of the CGBS, in addition to motion artifacts, can contain also residuals of gradient artifacts. This is,

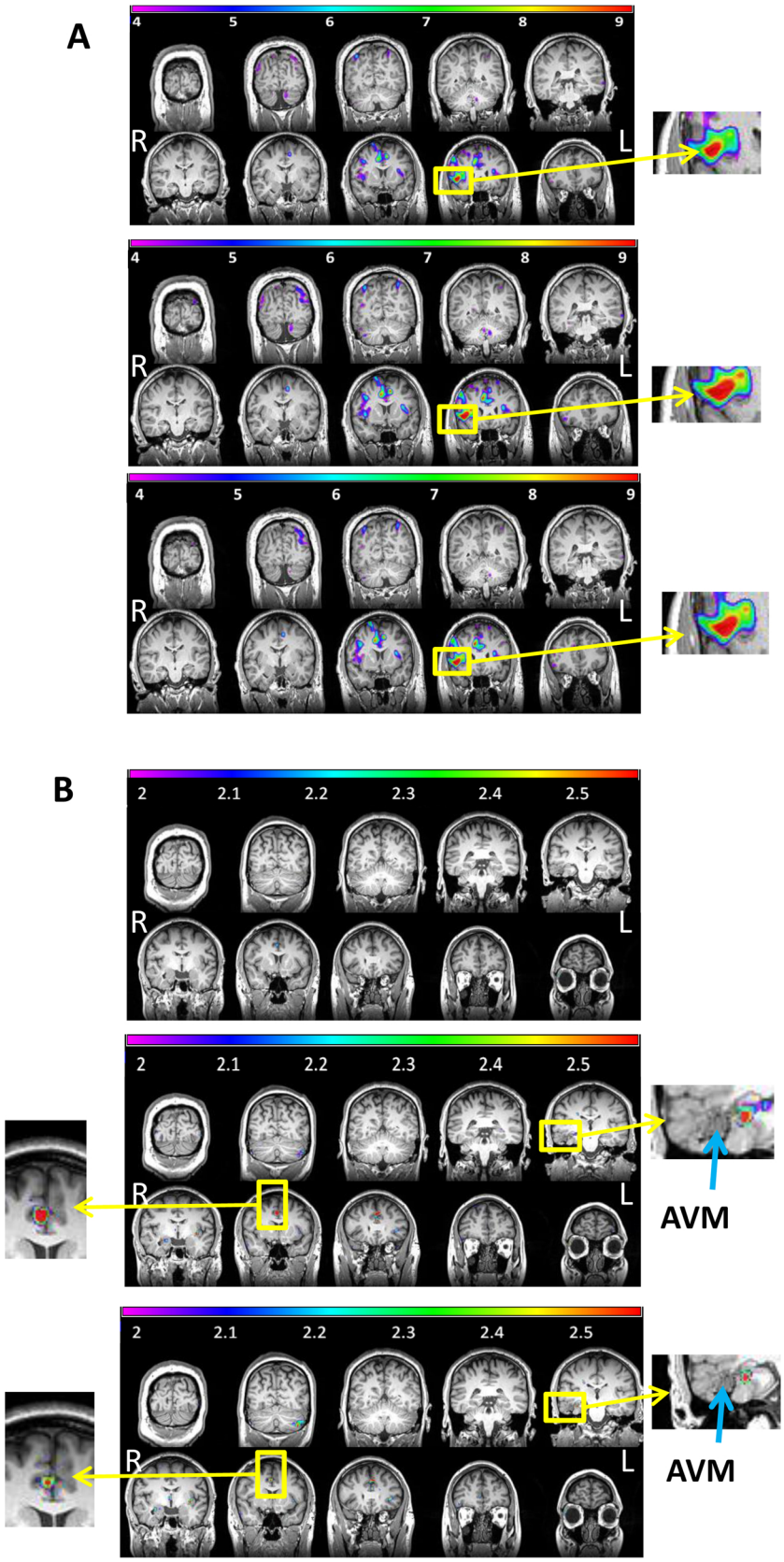

Fig. 3. Effect of CGBS based movement correction on BOLD analysis results. Three different techniques for cleaning movement artifacts were applied for comparison on data from patients 1(3 A) and 2(3B). IED related T-maps were thresholded at T = 4 and T = 2 and corresponded to 60 min and 40 min long scans, respectively. Peak BOLD activations are displayed and enlarged. IED related T-maps are shown using GLM without outlier regressors (top); with ART outlier regressors (middle); and with the CGBS based outlier regressors (bottom). The peak t-values and activation pattern resulting from ART and CGBS based analyses are similar. CGBS, conductive gel bridge sensor; BOLD, blood oxygen-level-dependent; IEDs, interictal epileptiform discharges; GLM, general linear model; AVM, arteriovenous malformation.

however, true for any type of motion sensor based on an electrically conductive loop.

It is important to note that CGBS, as other types of motion sensors based on cable loops, can be helpful in motion artifact detection (and probably suppression), however, the information obtained by CGBS cannot be used for updating the fMRI acquisition system online. This is in contrast to optic motion tracking systems (Körbl et al, 2016; Maziero et al., 2016), which can be used in prospective motion correction (PMC)

Table 1
Comparison of t values in areas of peak activity in presumed SOZ during IEDs associated with different motion cleaning methods.

	GLM without outlier regressors	GLM with ART outlier regressors	GLM with CGBS outlier regressors
Patient 1	T = 9.76	T = 10.79	T = 11.03
Patient 2	T = 1.5	T = 2.63	T = 2.56

using motion tracing information for updating radiofrequency and gradient fields with minimal delay.

Generally, the CGBS approach is based on electro-magnetic induction and can be most predictably used inside strong magnetic fields but not only for EEG-fMRI. For example, it can also be used as a breathing sensor during standard MRI recordings, when two ECG electrodes are interconnected by a conductive gel bridge. Regarding the possible use of CGBS in EEG measurements out of the MR-scanner, slow and small amplitude movements will not produce substantial change in the CGBS trace. The fast and large amplitude movements produced by head and/or EEG cables may possibly produce some signal captured by the CGBS out of the MR-scanner, but this requires further study. Since the motion artifacts recorded by CGBS and by EEG channels have similar telecourses (Fig. 2), artifact removal algorithms based on CGBS could also be implemented in the future in a similar manner previously described for other motion sensors based on conductive loops. For example, the multichannel recursive least squares method (Masterton et al., 2007) and/or independent component analysis (Jorge et al., 2015) can utilize information from the motion sensors to optimize the artifact removal process.

We conclude that an easy-to-apply gel bridge between two adjacent electrodes can create a conductive loop serving as a motion sensor for EEG-fMRI, available for immediate use with currently available setups.

Funding

This research was partially supported by the Tel Aviv Medical Center (TLVMC) BRAIN grant, the Sackler Faculty of Medicine graduate scholarship and the Ministry of Aliyah and Integration Scholarship Program. These funding sources had no involvement in study design, data collection and interpretation or in the decision to submit this work for publication.

Disclosure

Firas Fahoum, Talma Hendler and Mordekahy Medvedovsky are authors of a patent related to the dual array EEG-fMRI method (WO2012046237A2). Other authors report no conflict of interest.

Acknowledgements

We acknowledge the SensoMedical laboratories Ltd. team for their contribution to the construction of the EEG cap, particularly Shurooq Melhem, Luai Asfour and Maroon Farah. Prof. Dafna Ben-Bashat and Dr. Moran Artzi were involved in MRI protocol planning and configuration.

Appendix A. Supplementary data

Supplementary material related to this article can be found, in the online version, at doi:https://doi.org/10.1016/j.eplepsyres.2018.12.008.

References

Abbott, D.F., Masterton, R.A., Archer, J.S., Fleming, S.W., Warren, A.E., Jackson, G.D., 2014. Constructing carbon fiber motion-detection loops for simultaneous EEG-fMRI. Front. Neurol. 5, 260.
Bonmassar, G., Purdon, P.L., Jääskeläinen, I.P., Chiappa, K., Solo, V., Brown, E.N., Belliveau, J.W., 2002. Motion and ballistocardiogram artifact removal for interleaved recording of EEG and EPs during MRI. Neuroimage 16 (4), 1127–1141.
Chowdhury, M.E., Mullinger, K.J., Glover, P., Bowtell, R., 2014. Reference layer artefact subtraction (RLAS): a novel method of minimizing EEG artefacts during simultaneous fMRI. Neuroimage 84, 307–319.
Gotman, J., 2008. Epileptic networks studied with EEG-fMRI. Epilepsia 49 (Suppl. 3), 42–51.
Iannetti, G.D., Niazy, R.K., Wise, R.G., Jezzard, P., Brooks, J.C., Zambreanu, L., Vennart, W., Matthews, P.M., Tracey, I., 2005. Simultaneous recording of laser-evoked brain potentials and continuous, high-field functional magnetic resonance imaging in humans. Neuroimage 28 (3), 708–719.
Jorge, J., Grouiller, F., Gruetter, R., van der Zwaag, W., Figueiredo, P., 2015. Towards high-quality simultaneous EEG-fMRI at 7 T: detection and reduction of EEG artifacts due to head motion. Neuroimage 120, 143–153.
Klovatch-Podlipsky, I., Gazit, T., Fahoum, F., Tsirelson, B., Kipervasser, S., Kremer, U., Ben-Zeev, B., Goldberg-Stern, H., Eisenstein, O., Harpaz, Y., 2016. Dual array EEG-fMRI: an approach for motion artifact suppression in EEG recorded simultaneously with fMRI. Neuroimage 142, 674–686.
Körbl, K., Jacobs, J., Herbst, M., Zaitsev, M., Schulze-Bonhage, A., Hennig, J., LeVan, P., 2016. Marker-based ballistocardiographic artifact correction improves spike identification in EEG-fMRI of focal epilepsy patients. Clin. Neurophysiol. 127 (8), 2802–2811.
Luo, Q., Huang, X., Glover, G.H., 2014. Ballistocardiogram artifact removal with a reference layer and standard EEG cap. J. Neurosci. Methods 233, 137–149.
Masterton, R.A., Abbott, D.F., Fleming, S.W., Jackson, G.D., 2007. Measurement and reduction of motion and ballistocardiogram artefacts from simultaneous EEG and fMRI recordings. Neuroimage 37 (1), 202–211.
Maziero, D., Velasco, T.R., Hunt, N., Payne, E., Lemieux, L., Salmon, C.E.G., Carmichael, D.W., 2016. Towards motion insensitive EEG-fMRI: correcting motion-induced voltages and gradient artefact instability in EEG using an fMRI prospective motion correction (PMC) system. Neuroimage 138, 13–27.
Niazy, R.K., Beckmann, C.F., Iannetti, G.D., Brady, J.M., Smith, S.M., 2005. Removal of FMRI environment artifacts from EEG data using optimal basis sets. Neuroimage 28 (3), 720–737.
Smith, S.M., 2002. Fast robust automated brain extraction. Hum. Brain Mapp. 17 (3), 143–155.
Warach, S., Ives, J.R., Schlaug, G., Patel, M.R., Darby, D.G., Thangaraj, V., Edelman, R.R., Schomer, D.L., 1996. EEG-triggered echo-planar functional MRI in epilepsy. Neurology 47 (1), 89–93.